UNDERGROUND MINE NAVIGATION USING AN INTERGRATED IMU/TOF SYSTEM WITH UNSCENTED KALMAN FILTER

Khonzi Hlophe[1], and Jeremy Green[2]
[1] Novel Mining Methods Research Group
CSIR: Centre for Mining Innovations
Johannesburg, South Africa
e-mail1: hlophek@gmail.com
[2] Novel Mining Methods Research Group
CSIR: Centre for Mining Innovations
Johannesburg, South Africa
e-mail2: jgreen@csir.co.za

ABSTRACT

Platform pose (localization and orientation) information is a key requirement for autonomous mobile systems. The severe natural conditions and complex terrain of underground mines diminish the capability of most pose estimation systems, especially GPS. Our research interest is focused on using low-cost off-the-shelf IMU to improve the Active Beacon Positioning System (ABPS) developed here at the CSIR. This paper proposes a novel pose estimator, for underground mines, that fuses together data from the ABPS and low-cost MEMS based IMU. This pose estimator uses a square-root unscented Kalman filter (SR-UKF) to fuse the data together. The method is evaluated by building a complete system in a lab.
Keywords: Sensor fusion, Navigation, Unscented Kalman Filter, Estimation.

1 INTRODUCTION

South Africa plays a major role in the international mining fraternity. Mining employs 495 000 workers directly and a similar amount indirectly, providing a daily subsistence for approximately 5 million South Africans [1]. Robotics could aid the mining industry to achieve government safety standards. Some of the main challenges were discussed by Green and Vogt in [2].

Open-cast mines have long navigated vehicles using integrated GPS/INS systems. GPS is unavailable in underground mine environments, which means that another system has to be used. This paper gives a basic introduction to the positioning algorithm of an ultrasonic time-of-flight (TOF) based system. It further discusses the fusion of this system with an inertial measurement unit (IMU) using a square-root unscented kalman filter (SR-UKF).

2 PREVIOUS WORK

Van der Merwe and Wang [3] presented a dynamic process model which includes time varying bias terms. They used first-order Euler integration for state update and an UKF for state estimation. They successfully implemented the method to automate a model helicopter.

Zhang et al [4] introduced a new set of general dynamic models of IMU to describe the state of a automobile. These dynamic equations are, closely resemble the above method, integrated using a fourth-order Runge-Kutta approach instead of a first order Euler integration as in [3].

The contribution of this paper includes the use of the ABPS and the fully embedded application of the UKF. Our proposed system also differs by the use of the beacon distance in the measurement model, rather than the system's position. The UKF is used to fuse the data from the ABPS and the IMU. The UKF source code is optimized for the embedded application.

The next section discusses the localization system's different components and their functions. Section **Error! Reference source not found.** describes the localization algorithm using an unscented Kalman filter. Section **Error! Reference source not found.** describes the state vector, process model and measurement model. It further describes the UKF implementation. The final two chapters discuss the solution and provide the conclusion.

3 THE NAVIGATION SYSTEM

The system implementation diagram is given in *Figure **1***. The navigation system uses both relative sensors, in the form of an IMU, and absolute sensors, in the form of an active beacon positioning system. The main localization data fusion algorithm is an unscented Kalman filter [3], [5] that fuses the sensor data to estimate the pose. The process model describes the time evolution of the state and the measurement model provides the link between the measurements and the system state. The navigation system must provide localization within *10cm* at a moving speed of *0.5m/s*.

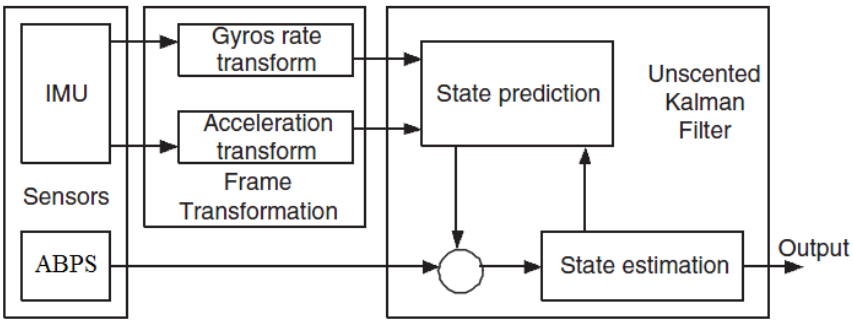

Figure 1: Figure Heading.

3.1 Inertial Measurement Unit (IMU)

The Inertial Measurement Unit (IMU) used in the project is the ADIS16364 from Analog Devices. This is a strap-down IMU with six degrees of freedom. The factory calibration characterizes the sensor for sensitivity, bias, alignment, and linear acceleration (gyro bias). As a result, each sensor has its own dynamic compensation formulas that provide accurate sensor measurements over a temperature range of -20^oC to $+70^oC$ [6].

The ADIS16364 was selected because it claimed to provide a simple, cost-effective method for integrating accurate, multiaxis inertial sensing into industrial systems, especially when compared with the complexity and investment associated with discrete

designs. All necessary motion testing and calibration are part of the production process at the factory, greatly reducing system integration time [6]. Tight orthogonal alignment simplifies inertial frame alignment in navigation systems.

3.2 Absolute Sensors

The dead reckoning Kalman filter can substantially reduce the localization error in measurement but, since the actual position and heading are unobservable [7], the filter will inevitably diverge. Absolute measurements are necessary to bind the dead reckoning localization error.

The active beacon positioning system (ABPS) developed is intended for excavations of the order of *30m X 3m X 1m* in tabular ore bodies, explained by Ferreira1 [8]. The environment is populated by a number of beacons with known positions. The Green Mamba only requires the distances between the receivers and the beacons and the position of the beacons to estimate the position.

3.2.1 Beacon Implementation

Beacons exist in a common environment and periodically transmit information that is utilized by any number of ABPS receivers within coverage. This information includes the synchronized ultrasonic and electromagnetic signals used for ranging, a form of unique identification and the beacon's own location. The location of a beacon is surveyed during installation and stored in memory on the beacon.

The radio signal is used for a number of functions. In the design, location and identification information are transmitted by the radio. Apart from transmitting a beacon's location and identification, the start of the transmission serves as the synchronization mechanism and during transmission the carrier is used to avoid transmission collisions. *Figure **2*** demonstrates the synchronization by the RF channel. The full beacon localization system was presented at CARSFOF 2010.

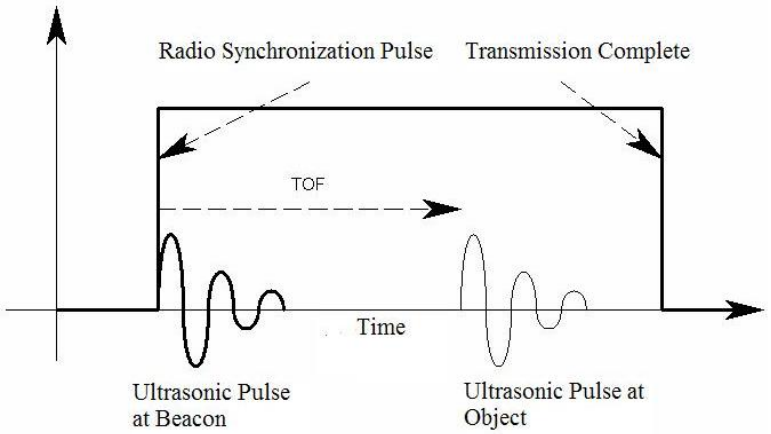

Figure 2: RF signal used as synchronization.

3.3 Data Logging and Processing Device

The system architecture consists of three major components: the relative localization, the absolute localization system and a data-logging and processing system. The data logging and processing is done using a Green Mamba single board computer. The Green Mamba is

a high performance embedded control board based on a modular architecture for easy expandability, which is designed and developed by the Council for Scientific and Industrial Research (CSIR). The board is based on the AVR 32 32-bit microcontroller 512 Kbytes flash memory. This gives the board high performance at low power consumption and runs on the FreeRTOS real-time embedded operating system. The board is equipped with a real-time clock with battery backup, micro-SD card interface, 10/100Mbps ethernet and 2.0 Full Speed and On-The-Go USB to name a few features.

4 LOCALIZATION ALGORITHM

A variety of sensors are available for the state estimation and each sensor has its own downfall, therefore a data fusion algorithm is required. The main localization data fusion algorithm is a discrete unscented Kalman filter (UKF) [3], [5] that fuses relative sensor observations and observations from the absolute sensors to estimate pose. The UKF will estimate the state recursively and iteratively in near real-time, constantly driving the uncertainty of the solution downwards.

4.1 The Square-root Unscented Kalman Filter

Since the classic Kalman filter requires the assumption that the process and measurement equations are linear in the state variables, a generalization of the Kalman filter must be used that can account for the non-linear quaternion measurement model. One approach is to approximate the non-linearities to first order using an Extended Kalman Filter (EKF), but this approach has been mostly replaced by sigma-point methods such as the Unscented Kalman Filter (UKF) [5]. Sigma-point filters pass a set of points representing the input distribution through the non-linear functions, and then approximate the output statistics. The UKF is accurate to third order for any nonlinearity, but only requires computational resources on par with the EKF [3].

Due to numerical round-off errors, it is possible for the state covariance matrix to cease to be positive definite, causing the UKF algorithm to fail when taking a square root of the covariance to calculate the sigma points. To prevent this possibility, the square root of the covariance matrix can calculated directly during every time step, without using the actual covariance matrix. The efficient implementation of van der Merwe and Wan makes use of Cholesky factor updating, allowing for better performance than even a normal UKF [3]. The equations from van der Merwe and Wan's paper are described below.

The filter is initialized with a mean vector and the square root of a covariance as follows

, (1)

. (2)

The Cholesky factorization decomposes a symmetric, positive-definite matrix into the product of a lower-triangular matrix and its transpose. This triangular matrix is used directly to calculate the sigma points:

. (3)

The scaling constant is calculated from

, (4)

where is a tunable parameter less than one. The sigma points are then passed through the nonlinear process model, which predicts the current state for each sigma point and the previous IMU data, .

. (5)

The estimated mean and square root covariance are calculated from the transformed sigma points using

, (6)

, (7)

(8)

where

– , (9)

, (10)

. (11)

The parameter α is the same as above, and β is another tunable parameter used to incorporate prior knowledge of the state distribution (β=2 is optimal for Gaussian distributions). The matrix is the process noise covariance. The QR factorization decomposes a matrix into the product of an orthogonal matrix and a triangular matrix; only the triangular matrix is used here. Since the zero weight may be negative, the separate Cholesky update operation is needed; the Cholesky update operation efficiently transforms the Cholesky decomposition of the matrix A into the Cholesky decomposition of the matrix A + , where is a row vector.

The transformed sigma points are then used to predict what measurements the sensors will make, using the nonlinear measurement model:

. (12)

The expected measurement and square root covariance of (the difference between the actual and expected measurements, also called the innovations) are given by the unscented transform equations just as for the process model:

, (13)

, (14)

. (15)

In order to determine how much to adjust the predicted mean and covariance based on the actual sensor input, the Kalman gain matrix is calculated:

, (16)

. (17)

Note that is square and triangular, so efficient back-substitutions can be used rather than a costly matrix inversion. Finally, the state mean and covariance are updated using the actual sensor input and the Kalman gain matrix:

(18)

, (19)
(20)

4.2 The Process Model

The system is implemented on an embedded platform and it is for this reason that we used the standard IMU driven kinematic process model formulation that comprises of an INS mechanization component [9], [10] and an IMU sensor error model component, similar to Zhang et al [4]. The IMU sensor error model components are added to our state vector because the low cost MEMS based IMU used in the system has a large bias and scale factor errors. The estimated values of these error components are then used to correct the raw IMU acceleration and gyro-rate measurements before they are used inside the INS mechanization equations of the process model [5]. The 16 dimensional state vector, x, of our system is defined as follows:

, (21)

where

(22)

and

(23)

represent the position and velocity respectively and

(24)

represents the system attitude in quaternion in the navigation frame (n-frame). is the IMU acceleration biases, and is the IMU gyro rate biases. van der Merwe [5] states that a time varying bias term is sufficient to model the combined effect of the bias and scale error terms and therefore eliminates the need to include the scale factor in the state vector.

The continuous time kinematic navigation equations, INS mechanization equations and error model discussed above, operating on this state vector and driven by the error corrected IMU measurements and can be established as:

(25)

In Equation 2, is the direction cosine matrix (DCM) transforming vectors from the body frame (b-frame) to the n-frame. The DCM is a nonlinear function of the current attitude quaternion and is given by

(26)

=2 . (27)

The is the gravity vector in the n-frame, which is expressed by

, (28)

where is the local gravity, which is decided by the coordinates in the geodetic coordinate system [11]. The raw measurements are defined as

, (29)
(30)

In the above equations, and are the raw measurements of acceleration and gyro-rates coming from the IMU, and and are the IMU acceleration and gyro-rate measurement noise, and is the rotation rate of the earth as measured in the navigation frame (n-frame) relative to the earth frame (e-frame) and hence is time-varying [5] as the n-frame moves relative to the e-frame. For terrestrial navigation, we assume the n-frame is stationary relative to the e-frame resulting in a constant for a given origin location, latitude and longitude, of the n-frame.

In Equation 2, is the IMU-lever-arm coupling component due to the IMU not being located at the center of gravity of the system. This component can be ignored if the navigation filter computes the state estimate at the IMU location [5]. This IMU centric navigation solution can then simply be transformed to the center of gravity location after the fact as needed by the control system.

One of the most common properties of IMU, despite their quality, is that the acceleration and gyro rate output are known to be in error by an unknown slowly time-varying bias [4]. Usually the turn-on bias is accurately known and accounted for in the IMU calibration. Since the bias and scale factor of low cost MEMS based IMU sensors exhibit non-zero mean and non-stationary behavior, the residual time-varying bias error is modeled as a random-walk process [11] in order to improve the tracking of these time-varying errors by the navigation filter. This does, however, require that the effect of these errors be observable through the specific choice of measurement model. Therefore, , and in Equation 2 are white noise of acceleration and gyro rate respectively in the IMU.

Equation 2 has to be discretized for implementation in the embedded system. The position and velocity discrete-time updates are calculated by the following simple first-order Euler updates [5]

(31)

(32)

where and are calculated using Equation 2 and dt is the integration time-step of the system, usually dictated by the IMU data rate. The quaternion propagation equation can be discretized with an analytical calculation of the exponent of the skew-symmetric matrix. The discrete-time update can be written as

– . (33)

If we further denote

(34)

(35)

(36)

as the effective rotations around the body frame (b-frame) or roll, pitch and yaw axes undergone by the system during the time period , assuming that the gyro-rates , and remained constant during that interval, we can re-introduce the 4 4 skew-symmetric matrix

(37)

(38)

Using the definition of the matrix exponent and the skew symmetric property of , we can write down the following closed-form solution [5]:

– – ——, (39)

where

– (40)

– (41)

Proof of this closed-form can be found in [5].Theoretically, Equations 3 and 4 ensure that the updated quaternion has a unit norm. It is common to add a small Lagrange multiplier term to the first component of Equation 4 to further maintain numerical stability and the unity norm of the resulting quaternion [5]. The resulting final solution for the time-update of the quaternion vector is given by

– —— (42)

where is the deviation of the square of the quaternion norm from unity due to numerical integration errors, and is the factor that determines the convergence speed of the numerical error. These factors serve the role of the above mentioned Lagrange multiplier that ensures that the norm of the quaternion remains close to unity. The constraint on the speed of convergence for the stability of the numerical solution is < 1 [12].

Finally, the discrete time random-walk process for the IMU sensor error terms are given by

(43)

(44)

where and are zero-mean Gaussian random variables.

4.3 The Measurement Model

If we assume that the robot moves slowly, the time-of-flight (TOF) measurements of the ultrasonic localization system are expressed using the following matrix equation

= (45)

where

In Equation 5, and denote the TOF and the time delay of the beacon, respectively. Measurement noises, in the same equation, are regarded as mutually independent, zero-mean white Gaussian processes with covariance

. (46)

Equation 5 can be more compactly rewritten in the vector-matrix form

(47)

where

, (48)

(49)
(50)

5 RESULTS AND DISCUSSIONS

The Green Mamba performs all the calculations in the experiment. In *Figure **3*** the Green Mamba single board computer is on the left. The Green Mamba communicates with the IMU via SPI with the Green Mamba being the master and the IMU being the slave. The Green Mamba and the ABPS, bottom right component in *Figure **3***, communicate via UART based on a RS232 protocol.

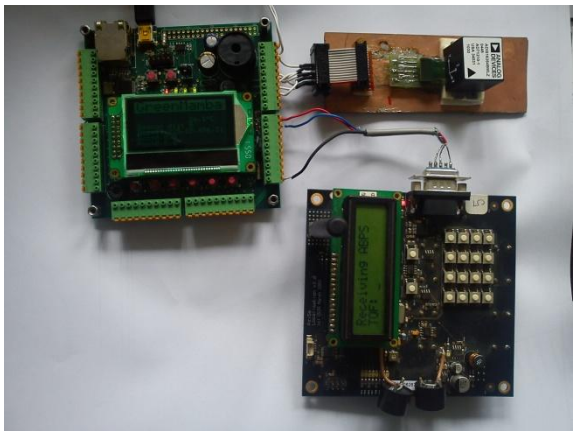

Figure 3: Experimental Setup with IMU, ABPS and Green Mamba

The required processing is too heavy for an embedded system. FreeRTOS allows tasks to run, virtually, concurrently. This feature is useful as it allows us to run the UKF in a pseudo-off-line state. This means we let the Green Mamba perform its normal tasks including capturing data from the navigation sensors, among other tasks. FreeRTOS also allows the user to set the task priority. By decreasing the priority of the UKF task, the Green Mamba can continue to perform the data collection and control tasks while the UKF task runs in the background.

The Green Mamba streams data to a PC over RS-232. The practical experiment is a typical low-speed test. The Green Mamba was powered on with the y axis pointing straight up. A series of rotations were performed on the x-axis, then rotations were performed on the z-axis, and finally (after one-half x-axis rotation to reset to the initial position) rotations were performed on the y-axis.

We compared the actual data and the results of the measurement prediction step in the SR-UKF for verification of the filter. *Figure **4*** shows the estimated state can generate measurement predictions that closely match the IMU data. This is strong evidence of the fidelity of the measurement model.

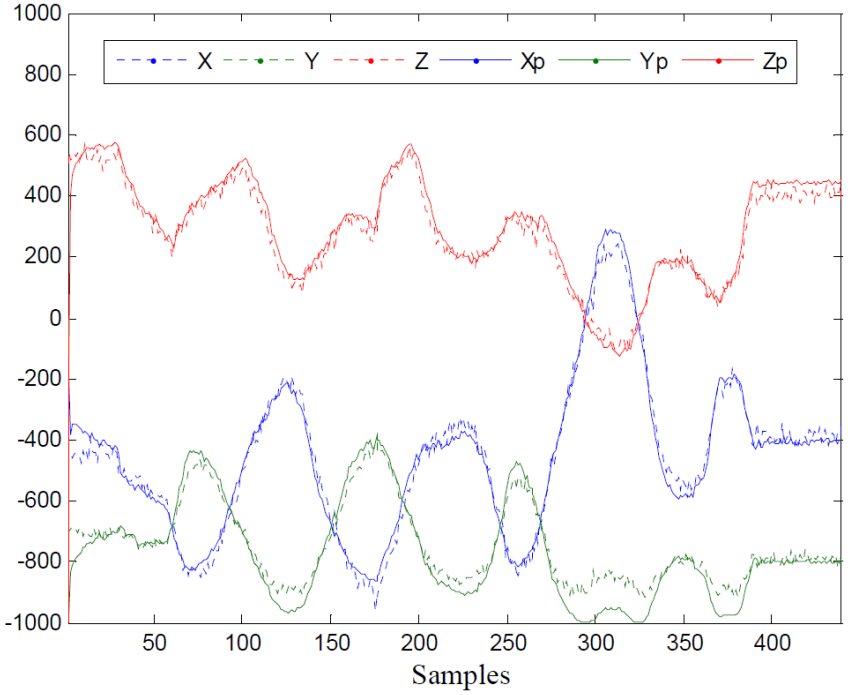

Figure 4: Actual vs. Predicted Measurements.

6 CONCLUSION

We present an underground navigation method by integrating the measurements of IMU and ABPS. The measurement of an IMU is based on the inertial frame (i-frame) while the measurements of the ABPS are based on the n-frame. So the standard IMU driven kinematic model used for the system include the associated transformations from the i-frame to the n-frame. The system state estimation is implemented using the SRUKF for its computational advantage against the UKF. This system was evaluated in a lab at the CSIR. The measurement predictions closely resemble the actual measurement

7 RECOMMENDATIONS

The immediate progression in the research is to characterize the system efficiency and accuracy. The data will be post processed on the Green Mamba. This will allow us to capture all the data from the sensors and the results of the filter. The accuracy will be compared to the Matlab implementation of the filter developed for technique verification. Saving the data will also verify the reliability of the system by checking the repeatability of the experiments. Finally the efficiency of the technique will be characterized. The Green Mamba has a built-in real-time clock which can be used to measure the processing time and track improvements made in the code.

8 ACKNOWLEDGEMENTS

The authors would like to thank the Centre for Mining Innovations (CMI) of the Council for Scientific and Industrial Research (CSIR) in South Africa for funding this work.

9 REFERENCES

[1] J. J. Green, P. Bosscha, L. Candy, K. Hlophe, S. Coetzee, and S. Brink, Can a robot

improve mine safety?, in 25th International Conference of CAD/CAM, Robotics & Factories of the Future, Pretoria, 2010.

[2] J. J. Green and D. Vogt, Robot miner for low grade narrow tabular ore bodies: the potential and the challenge, in 3rd Robotics and Mechatronics Symposium (ROBMECH 2009), in 25th International Conference of CAD/CAM, Robotics & Factories of the Future, Pretoria, 2010.

[3] R. Van der Merwe and E. Wan, Efficient derivative-free Kalman filters for online learning, in Proceedings of the 9th European Symposium on Artificial Neural Networks (ESANN), Bruges, IEEE, 2001.

[4] P. Zhang, J. Gu, E. E. Milios and P. Huynh, Navigation with imu/gps/digital compass with unscented Kalman filter, in International Conference on Mechatronics & Automation, IEEE press, 2005.

[5] R. van der Merwe, Sigma-point Kalman filters for probabilistic inference in dynamic state-space models, PhD dissertation, OGI School of Science & Engineering at Oregon Health & Science University, 2004.

[6] ADIS16364 six degrees of freedom inertial sensor, Analog Devices Inc., Norwood USA, 2010.

[7] B. Barshan and H. F. Durrant-Whyte, An inertial navigation system for mobile robot, in Proceedings of the 1993 IEEE/RSJ International Conference on Intelligent Robots and Systems, 1993.

[8] G. Ferreira, An implementation of an ultrasonic time-of-flight based localization, in 2nd International Conference on Wireless Communication in Underground and Confined Areas, 2008.

[9] P. G. Savage, Strapdown inertial navigation integration algorithm design part 1: Attitude algorithms, in Journal of Guidance, Control, and Dynamics, 1998.

[10] P. G. Savage, Strapdown inertial navigation intergration algorithm design part 2: Velocity and position algorithms, in Journal of Guidance, Control, and Dynamics, 1998.

[11] J. A. Farrell and M. Barth, The global positioning system & inertial navigation, McGraw-Hill, 1998.

[12] V. Gavrilets, Autonomous aerobatic maneuvering of miniature belicopters: Modelling and control, PhD. Dissertation, MIT, 2003.